




Research Article

Green Synthesis of Iron Nanoparticles from Spinach Leaf and Banana Peel Aqueous Extracts and Evaluation of Antibacterial Potential

Pankaj Kumar Tyagi ¹, Samridhi Gupta,¹ Shruti Tyagi,² Manoj Kumar ³,
R. Pandiselvam,⁴ Sevgi Durna Daştan,^{5,6} Javad Sharifi-Rad ⁷, Deepak Gola,¹
and Arvind Arya¹

¹Noida Institute of Engineering and Technology, Greater Noida, 201306 Uttar Pradesh, India

²Young Scientist of UPCST Scheme, Department of Biotechnology, Noida Institute of Engineering and Technology, Greater Noida, 201306 Uttar Pradesh, India

³Chemical and Biochemical Processing Division, ICAR-Central Institute for Research on Cotton Technology, Mumbai 400019, India

⁴Division of Physiology, Biochemistry and Post-Harvest Technology, ICAR-Central Plantation Crops Research Institute (CPCRI), Kasaragod, 671 124 Kerala, India

⁵Department of Biology, Faculty of Science, Sivas Cumhuriyet University, 58140 Sivas, Turkey

⁶Beekeeping Development Application and Research Center, Sivas Cumhuriyet University, 58140 Sivas, Turkey

⁷Facultad de Medicina, Universidad del Azuay, Cuenca, Ecuador

Correspondence should be addressed to Pankaj Kumar Tyagi; pktgenetics@gmail.com and Javad Sharifi-Rad; javad.sharifirad@gmail.com

Received 20 August 2021; Accepted 14 November 2021; Published 29 November 2021

Academic Editor: José Agustín Tapia Hernández

Copyright © 2021 Pankaj Kumar Tyagi et al. This is an open access article distributed under the Creative Commons Attribution License, which permits unrestricted use, distribution, and reproduction in any medium, provided the original work is properly cited.

Spinacia oleracea (spinach) and *Musa acuminata* (banana) were chosen for the study, and aqueous extracts of spinach leaf extract (SLE) and banana peel extract (BPE) were prepared for the synthesis of iron nanoparticles (FeNPs), and their antibacterial potential against pathogenic bacteria *Bacillus subtilis* (MTTC 1133) and *Escherichia coli* (MTTC 62) was evaluated. In 10 minutes at 60°C, the color of the mixture (FeCl₃+SLE) changed from light green to dark blackish-brown, and the color of the mix (FeCl₃+BPE) changed from transparent yellow to dark black, confirming the synthesis of FeNPs from SLE and BPE, respectively. The UV-Vis spectra of spinach- and banana-derived FeNPs revealed two peaks ranging from 240 to 430 nm and multiple peaks at 240, 270, and 395 nm, respectively. FTIR spectroscopy was used to show different functional groups on BPE and SLE, and their role in FeNP synthesis was predicted. TEM micrographs showed that the particles were in nanoscale, ranging in size from 20 to 50 nm for BPE-derived FeNPs and 10 to 70 nm for SLE-derived FeNPs. The FeNP (BPE and SLE) XRD analysis revealed amorphism, with a weak iron characteristic peak, indicating noncrystallinity. The antibacterial potential of BPE- and SLE-FeNPs was investigated, and inhibition zones (mm) against *B. subtilis* (22.70 ± 0.4) and *E. coli* (20.45 ± 1.66) were observed, as well as SLE-FeNPs against *B. subtilis* (23.56 ± 1.00) and *E. coli* (20.33 ± 0.58). There were no significant differences in antibacterial activities between BPE-FeNPs and SLE-FeNPs. Positive controls were tetracycline and gentamicin, both standard antibiotics, at 5 µg/disk. SLE- and BPE-derived green FeNPs were also analysed *in vivo* of *D. melanogaster* life history traits, i.e., fecundity, hatchability, viability, and duration of development for toxicity evaluation. SLE- and BPE-derived green FeNPs at a concentration of 10 mg/L were fed flies compared to normal diet-fed flies (control sample), and no significant differences were observed between them. The findings suggest that FeNPs have a high antibacterial potential and could be used as antibacterial agents against pathogenic bacteria while being nontoxic in nature.

1. Introduction

Nanotechnology is the manipulation of matter through chemical and/or physical processes to produce materials with specific properties that can be used in multifaceted applications [1]. A nanoparticle (NP) is a microscopic particle with at least one dimension smaller than 100 nm in diameter [2, 3]. NPs have unique optical, thermal, electrical, chemical, and physical properties [4, 5], and as a result, they have a wide range of applications in medicine, chemistry, the environment, energy, agriculture, information and communication, heavy industry, and consumer goods [6–8]. Attrition and pyrolysis, for example, are traditional NP synthesis methods with drawbacks such as defective surface formation, low production rate, and high manufacturing costs with high energy requirements [9]. Toxic chemicals are used in chemical synthesis methods (e.g., chemical reduction and sol-gel technique), as well as the formation of hazardous by-products and contamination from precursor chemicals [10, 11]. As a result, there is a growing need to develop clean, nontoxic, and environmentally friendly NP synthesis procedures. Biological synthesis protocols have several distinct advantages over traditional physical and chemical methods: (i) nontoxic chemicals are not used, making this a clean and environmentally friendly method [12–15]; (ii) the active biological component, such as an enzyme, acts as a reducing and capping agent, lowering the synthesis process' overall cost [15]; (iii) even in large-scale production, small NPs can be produced [16]; and (iv) external experimental conditions such as high energy and high pressure are unnecessary, resulting in significant energy savings [17]. For NP synthesis, a wide range of biological resources such as microorganisms (bacteria, yeast, fungi, algae, and viruses) and plants can be used [18]. Plant-mediated biological synthesis of NPs has only recently gained importance [19], whereas microbe-based protocols have been developed from the combined research efforts of several authors. Plant extracts, as opposed to microbes, reduce metal ions in a shorter time. NPs can be made in a matter of minutes or hours, depending on the plant type and phytochemical concentration, whereas microorganism-based methods take longer [20]. The main disadvantage of microbe-mediated NP synthesis is the requirement for aseptic conditions, which requires trained personnel and raises the scaling-up cost [21]. Plants are preferred biological resources over microbes for all of these reasons and the ease of finding them in nature. Magnetic NPs have risen to prominence as a new class of important nanoparticles with unique properties such as superparamagnetism and high coercivity. When made with traditional methods, these NPs have some drawbacks. At such tiny levels, conventional rules of physics and chemistry become dormant and inactive. Iron NPs are submicrometer particles of iron metal. NPs are highly reactive because of their large surface area. Iron NPs retain the magnetic properties of the metal iron. Due to its large surface area, iron NPs find their application in medical imaging, MRI [22], and targeted drug delivery [23] and help in treating several neurodegenerative diseases such as Alzheimer's disease. Iron NPs are also used to scour organic pollutants

in groundwater. Conventionally, NPs were synthesized by physical [24] and chemical [25] methods.

The green synthesis of iron NPs from plant extract is under exploitation and a better process than culturing cells of microorganisms. The green synthesis of iron NPs has gained interest for its nontoxicity [26] and is inexpensive to synthesize. It is an ecofriendly method as it does not use any harmful chemicals. Iron NPs are very efficient and promising to reform many environmental issues. In this research, spinach leaf extract and banana peel are considered for the production of iron NPs. *Spinacia oleracea*, commonly known as spinach, is a leafy green plant that belongs to the family of Amaranthaceae and is a superfood as it has lots of nutrients that are beneficial to humans [27]. It is an excellent source of iron and contains 0.81 g of iron. It also provides vitamins, proteins, and minerals. Banana is the most stand-out fruit in the world, and it belongs to the family *Musaceae*; banana peels are the outer covering of the banana and are also known as banana skin. It forms 18–30% of the whole banana [28]. Banana peels have diverse compounds which contain phenol that can act both as reductant and coating agents and can be used in the green synthesis approach [28]. It also includes a huge quantity of phenols that helps in the production of metallic NPs. As banana peels are not consumed and are thrown in the garbage as waste in heaps, it becomes necessary to find their applications to be used for the betterment of the environment. Promoting plant extracts over synthetic and chemical methods is very admirable as it gives way to green technology. It does not require any usage of high pressure or high temperature. The objective of this research paper is a green synthesis of iron NPs using spinach leaves and banana peel and their use as a potential antimicrobial agent against pathogenic bacteria as well as evaluating their toxicity *in vivo* on *Drosophila melanogaster* fruit fly.

2. Materials and Methods

2.1. Materials. Iron (III) chloride (ferrous chloride) was acquired from Central Drug House (P) Ltd. CDH, which was obtained and used without further decontamination. The ultrapurified and distilled deionized water (DDW) was obtained from the Institute's molecular biology laboratory. *M. acuminata* (banana) were collected from dumping sites, and *Spinacia oleracea* (spinach) was obtained from a local market.

2.2. Preparation of Aqueous Extract. The spinach leaf extract (SLE) and banana peel extract (BPE) were used to make aqueous extracts. Spinach leaves were collected and thoroughly cleaned with distilled water to ensure that they were free of dirt. Using a mortar and pestle, about 20 g of fresh leaves were weighed and crushed. To make the plant extract, 20 g of leaves were boiled in 100 mL deionized water for 20 minutes and magnetically stirred at 60°C and then filtered through filter paper. The extract was kept in the fridge for later use. About 100 g of fresh banana peels was collected, washed thoroughly with distilled water, cut into fine pieces, and vacuum dried for the banana peel extract. The dry

banana peel powder (8.3 g) was extracted with 125 mL DDW and stirred for 30 minutes at 60°C. Before filtering, the concentrate was allowed to cool. The samples were centrifuged for 30 minutes at 8000 rpm after extraction. Before use, the supernatant was collected, filtered, and stored at -20°C [29].

2.3. Biosynthesis of Iron Nanoparticles (FeNPs). SLE-FeNPs were made by dissolving the FeCl₃ in 40 mL of deionized water; a 0.1 M FeCl₃ solution was created. FeNPs were synthesized by mixing a 2:1 volume ratio of 0.1 M FeCl₃ solution with aqueous SLE at 60°C for 30 minutes with continuous magnetic stirring. As the Fe⁺³ ions decrease, the black color appears. The reaction mixture was prepared in 2:1 ratios, and the maximum absorption wavelengths of FeNPs in the UV/visible region were recorded. The BPE-FeNPs were made using a 2:1 volume ratio of 0.1 M FeCl₃ solution and aqueous BPE (supernatant at ambient temperature). After that, the mixture was hand-shaken for 1 minute and allowed to sit at room temperature for 1 hour. After 10 minutes, the solution color changed from transparent yellow to dark black, which was noted and recorded. The supernatant was poured out after centrifuging the mixture at 8000 rpm for 30 minutes. The black paste was redispersed in ethanol to remove any remaining biological molecules before being washed with ultrapurified water. To completely purify the NPs, the centrifugation and redispersion in ethanol and ultrapurified water process were repeated three times. The light black paste was then oven-dried overnight at 60°C, packed, and stored for characterization.

2.4. Characterization of Biosynthesized Iron Nanoparticles

2.4.1. UV-Vis Analysis. The changes in the reaction mixtures were observed visually and recorded. The sample was then spectrophotometrically examined in the UV-Vis range. The wavelength was scanned at 1 nm intervals from 200 to 700 nm. The instrument was turned on and given ten minutes to initialize. The sample solutions were placed in a quartz cuvette (1 cm), and the baseline was adjusted using ultrapurified water as the baseline. In the wavelength range of 200 to 700 nm, the spectra of extract, FeNPs, and ferric chloride solutions were obtained.

2.4.2. FTIR Analysis. An FTIR system was used to make the measurements. The extract functional groups that may have played a role in the synthesis of iron microstructures were identified using FTIR scans of iron NPs and both extracts. The transmission mode range of 400–4000 cm⁻¹ was used for the FTIR analysis.

2.4.3. Transmission Electron Microscopy (TEM). A TEM microscope with a 200 keV acceleration voltage was used to create the TEM images. The FeNP sample solutions were sonicated for 20 seconds in analytical grade methanol before being mounted on a carbon-coated copper grid with a mesh size of 200. The cleaned Teflon block was placed face-up on the treated grid, and 10 L of the NP sample solution was poured onto the grid and dried under an infrared lamp before the grid was loaded onto the microscope for measure-

ments. The average particle size was calculated and recorded using FeNP samples randomly selected from TEM images.

2.4.4. XRD Analysis. An X-ray diffractometer was used to examine crystalline metallic iron NPs. The instrument used Cu K α radiation at 45 kV and a monochromatic filter with a 20-80-degree wavelength range. Before being stacked in the cubes of the XRD equipment, the biosynthesized FeNPs were thoroughly dried to powder form.

2.5. Antibacterial Potential. The antibacterial potential of biogenic FeNPs derived from BPE and SLE was tested using the agar well diffusion method against two bacterial strains: *Bacillus subtilis* (MTTC 1133) and *Escherichia coli* (MTTC 62) obtained from the Microbial Type Culture Collection and Gene Bank (MTCC), Chandigarh, India, and the zone of inhibition was measured in millimeters using the agar well diffusion method described by Thiyagarajan et al. [7, 30–32]. Antibiotics such as chloramphenicol and gentamicin were used as positive controls in the study.

2.6. Impact of SLE- and BPE-Derived FeNPs on *Drosophila melanogaster*. *Drosophila melanogaster* was chosen in this investigation to identify if SLE- and BPE-derived green FeNPs had any toxic effects on life cycle traits. *D. melanogaster* were grown at 25°C on cornmeal, sucrose, agar-agar, dry yeast, live yeast, propionic acid, and sodium benzoate in a normal cornmeal feeding medium [7, 33]. After being combined in distilled water, all food components were boiled in appropriate cooked semisolid medium. The SLE- and BPE-derived green FeNP-treated food media were given to *D. melanogaster* at 10 mg/L concentrations, whereas the control sample was given only normal food medium as diet. Fecundity (the capacity to lay eggs), hatchability (the ability to bring forth from the egg), viability (larvae matured into adult fly), and development time (the time it takes for eggs to grow into adults) were all examined in *D. melanogaster* life cycle traits. In this investigation, ten replicates were carried out.

2.7. Statistical Analysis. The data in this paper were analysed using Statistica 7.0, an advanced analytics software system.

3. Results and Discussion

3.1. Visual Inspection of the Formation of the Iron Nanoparticles. The FeCl₃ solution and the aqueous extract solution from SLE and BPE were used to synthesize FeNPs, as shown in Figure 1. The color of the mixture (FeCl₃+SLE) changed from light green to dark blackish-brown and (FeCl₃+PBE) transparent yellow to dark black in 10 minutes at 60°C, demonstrating the synthesis of FeNPs from SLE and BPE (Figure 1). The surface plasmon vibrations of the FeNPs were excited, resulting in a dark color.

3.2. UV-Vis Analysis. The UV-Vis spectrophotometric method was used to examine the NPs first. Visual and UV-visible spectroscopy was used to monitor the formation of iron NPs. The wavelength was scanned from 200 to 700 nm, and the spectra obtained two peaks at 240 and

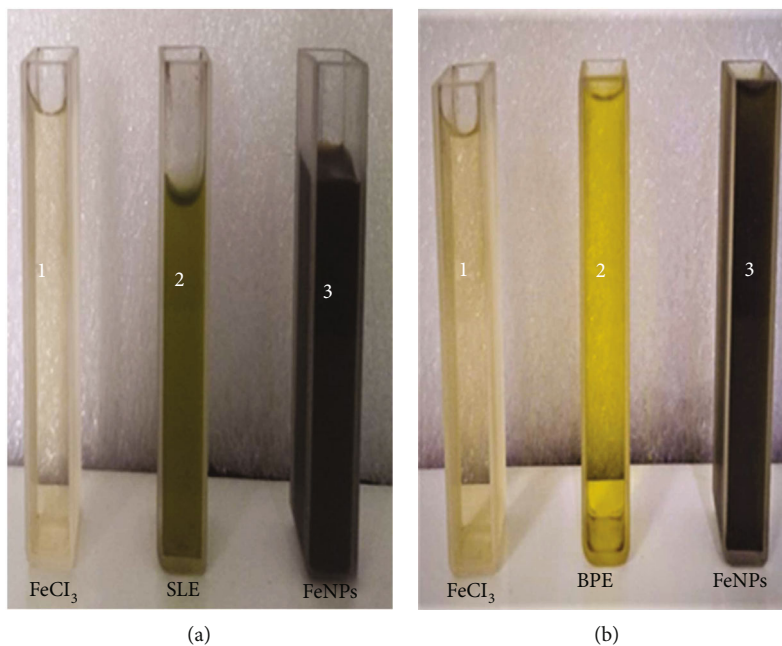


FIGURE 1: Visual inspection of the color changes indicating formation of FeNPs: (a) spinach leaf extract (SLE); (b) banana peel extract (BPE).

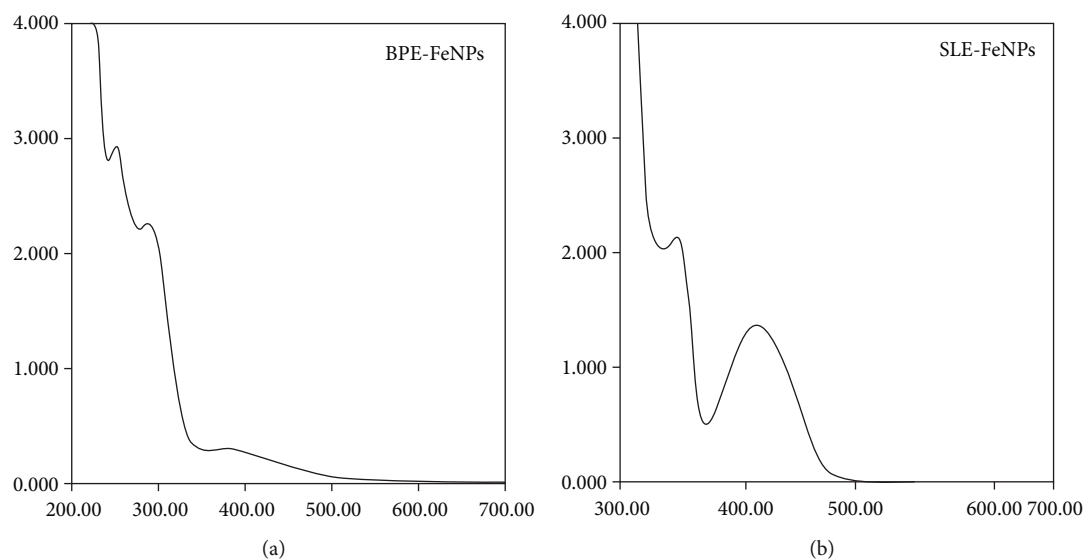


FIGURE 2: UV-visible spectra of BPE-FeNPs (a) and SLE-FeNPs (b).

430 nm and multiple peaks start from 240, 270, and 395 nm of the spinach- and banana peel-derived FeNPs (Figure 2). Peaks from 210 to 270 nm could indicate the presence of polyphenols in the solution, while peaks above 270 could indicate the presence of FeNPs in the solution. The biosynthesis of APE-FeNPs was confirmed with polyphenol peaks (237 nm, 272 nm) detected as biological components [34]. Eucalyptus leaf extract was utilized to synthesize FeNPs; similar results on visual observations and a peak around 276 nm have been reported [35]. The optimal conditions for synthesizing iron NPs in this study were pH 5.0 and a temperature of 90°C when 10 mg of BPEs were mixed with 1 mM of FeCl_3 [35].

The peak denoting O-H stretching in phenol was decreased (phenolic compound was used for the synthesis of FeNPs).

3.3. FTIR Analysis. Different functional groups on BPE and SLE were shown using FTIR spectroscopy, and their role in iron NP synthesis was predicted (Table 1). The O-H stretch at 3318 cm^{-1} was attributed to the O-H stretch in phenols present in the extract of BPE based on the FTIR spectra, and it decreases in FTIR of FeNPs. It may be assumed that these phenolic compounds were used for the synthesis of FeNPs. The O-H stretching in carboxylic acids was attributed to the peak in the BPE at around 2508 cm^{-1} . The

TABLE 1: FTIR peak position wavenumber (cm^{-1}), indicating different functional groups and concluding remarks of extract and FeNPs.

Sample	Peak position wavenumber (cm^{-1})	Peak assignment	Concluding remark of extract FTIR	Concluding remark of FeNP FTIR
BPE	(i) 3318	O-H stretching in phenol	(i) Peak denoting O-H stretching in phenol	(i) Peak denoting O-H stretching in phenol and was decreases (phenolic compound was used for the synthesis of FeNPs)
	(ii) 2508	O-H stretching in carboxylic acid	(ii) Peak denoting O-H stretching in carboxylic acid	(ii) Peak denoting O-H stretching in carboxylic acid was decreased
	(iii) 2131	Nitrile group	(iii) A strong and boarding peak was present, denoting nitrile group presence	(iii) A strong reduction was observed in this peak, and this group may possibly participate as a capping in the FeNPs
	(iv) 685	C-H stretching of aromatic	(iv) A weak peak denoting C-H stretching of aromatic was present	(iv) The absence of C-H stretching of aromatic peak and this may be conclude its involvement in the synthesis of FeNPs
	(v) 639	Strong peak of FeNPs	(v) This peak was absent	(v) A strong peak was observed and attributed to nanoparticles vibrations; this further confirmed the synthesis of the nanoparticles
SLE	(i) 3418	O-H stretching vibrations	(i) A strong and boarding peak with O-H stretching in phenolic compounds	(i) Shift towards higher frequencies and suggestion that polyphenol chemicals in the extract may be linked to the O-H group in the reduction process
	(ii) 2917	O-H stretching vibrations	(ii) O-H stretching vibrations	(ii) O-H stretching vibration of phenol groups, which might be responsible for the formation and stabilization of FeNPs
	(iii) 1620	C=O stretching vibrations	(iii) A strong peak was present representing higher amount of carbonyl group compound	(iii) This peak was very weak and only represents the very least amount of presence of carbonyl compound
	(iv) 1438	O-H bending vibrations	(iv) A weak peak was present	(iv) Bioreduction of ferric chloride into FeNPs and extract work as capping material
	(v) 540	Fe stretches in ferrous chloride	(v) This peak was absent	(v) A strong peak at 540 was attributed to nanoparticle vibrations confirming the production of nanoparticles
	(vi) 460	Fe stretches in ferrous chloride	(vi) This peak was absent	(vi) A strong peak at 460 was attributed to nanoparticle vibrations confirming the production of nanoparticles

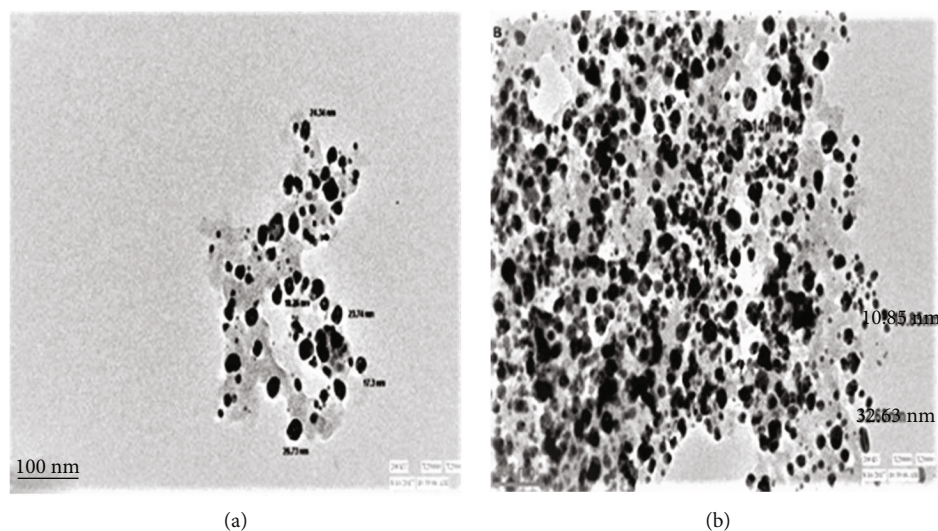


FIGURE 3: Images of transmission electron microscopy (TEM) to investigate the synthesis of nanoparticles in order to determine their morphology and size: (a) BPE-FeNPs; (b) SLE-FeNPs.

decrease in peak intensity in the FeNP spectra indicated that these groups might be involved in the NP synthesis process. The intensity of the nitriles stretched at 2131 cm^{-1} in the BPE decreased, indicating that nitrile groups in the BPE concentrate may be involved in FeNP capping. The presence of the C-H stretch of aromatics at 685 cm^{-1} in the BPE spectrum and the absence of the same peak in the FeNP spectrum indicated that it was involved in NP synthesis. The strong peak at 639 cm^{-1} was attributed to FeNP vibrations, which further confirmed the NP synthesis and absence in the extract FTIR of BPE. When these findings were compared to prior studies [36, 37], it was determined that FTIR from banana peel extract and FeNPs produced identical results. The possible biomolecules responsible for reducing FeNPs and capping of the bioreduced FeNPs synthesized by the SLE were identified using FTIR analysis. In the extract FTIR of SLE, a strong and prominent peak with O-H stretching in phenolic chemicals was found at 3418 cm^{-1} . In the FTIR of FeNPs, the shift towards higher frequencies indicated that polyphenol compounds in the extract may be connected to the O-H group in the reduction process. O-H stretching vibrations were also detected at 2917 cm^{-1} in the extract FTIR of SLE, and this O-H stretching vibration of phenol groups was responsible for the synthesis and stabilization of FeNPs. There was a stretching vibration of C=O groups in ketones, aldehydes, and carboxylic acids, and a strong peak was present at 1620 cm^{-1} in the extract, representing a higher amount of the carbonyl group compound, and this peak was extremely weak, only indicating the existence of a very little amount of the carbonyl compound in FTIR of FeNPs. The extract had a weak absorption peak at 1438 cm^{-1} , which could be responsible for the bioreduction of ferric chloride into FeNPs, and the extract works as a capping material. In the FTIR of FeNPs, absorption bands at 540 cm^{-1} and 460 cm^{-1} were found, which correspond to the Fe stretches in ferrous chloride and were attributed to nanoparticle vibrations, indicating the formation of nanoparticles. The SLE extracts did not include these two peaks.

According to FTIR analysis, the bioreduction of ferric chloride into iron NPs is due to the reduction of the spinach leaf extract by capping material [38, 39]. When these findings were compared to previous reports [40–42], it was discovered that the hydroxyl, carboxyl, and amide groups in BPE might be involved in the NP synthesis process.

3.4. Transmission Electron Microscopy (TEM). The transmission electron microscopy (TEM) method investigated the synthesized nanoparticles to determine their morphology and size [43]. The results are shown in Figure 3. According to TEM micrographs, the biologically synthesized iron NPs (SLE and BPE) are granular and dispersed throughout the grid. The particles are nanoscale, ranging from 20 to 50 nm for BPE-derived FeNPs to 10 to 70 nm for SLE-derived FeNPs. Using different plant extracts, similar iron NP results were obtained [44–50]. Despite being much larger than the 50 nm for FeNPs synthesized from tea extracts [34, 51–53] and *Couroupita guianensis* (cannonball tree), the 17 nm NPs were obtained [54], and this size range was more similar in size to NPs synthesized from Damask rose, with average sizes of 100 nm; *Thymus vulgaris* (garden thyme); and *Urtica dioica* (nettle leaf) [55].

3.5. X-Ray Diffractometer Analysis (XRD). The XRD analysis in Figure 4 shows that the synthesized FeNPs (BPE and SLE) were amorphous, with a weak characteristic peak of iron, indicating that the iron NPs were noncrystalline. In BPE-derived FeNPs, crystal planes of (110), (200), and (112) were responsible for the intense peaks observed at Bragg reflection $2\theta = 18.15^\circ$, 24.64° , and 35.78° , whereas in SLE-derived FeNPs, only one clear crystal plane of (112) and some fused crystal planes were responsible for the intense peaks observed at Bragg reflection $2\theta = 47.55^\circ$ (Figure 4). To confirm the presence of FeNPs, the Miller indices were used. Scherrer's formula was used to calculate the crystallite sizes: $D = K\lambda/\beta \cos \theta$, where D is the crystallite size, K is a constant of 0.94, λ is the X-ray wavelength, β is the half-width

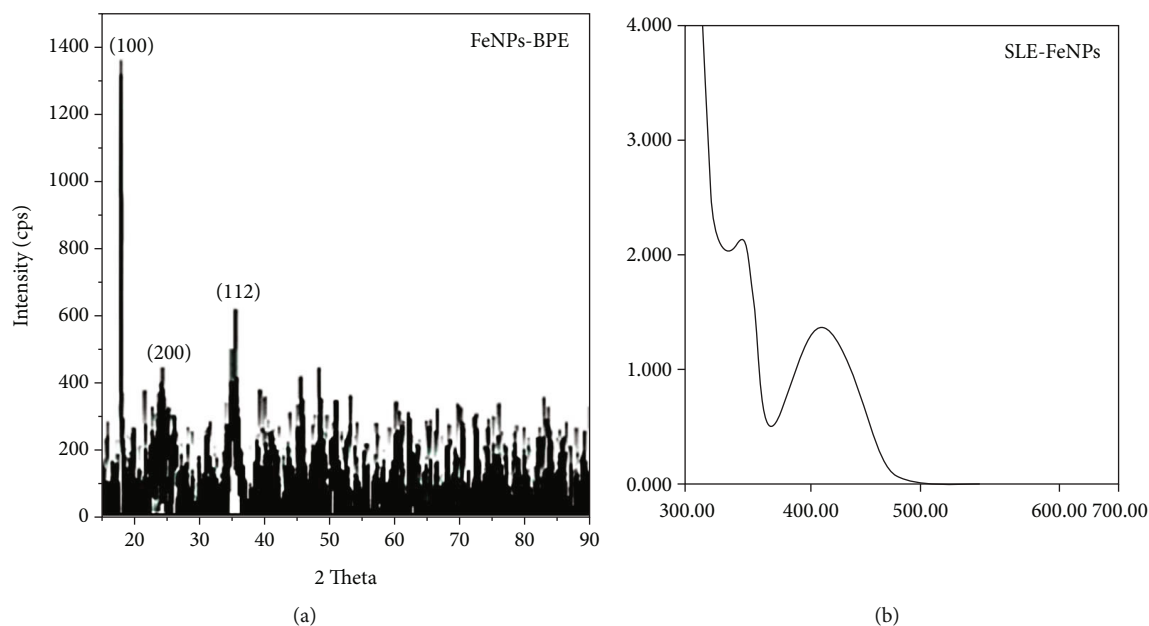


FIGURE 4: XRD spectrum of biological synthesized BPE-FeNPs (a) and SLE-FeNPs (b).

TABLE 2: Antibacterial potential of biogenic iron nanoparticles synthesized from BPE and SLE extracts against *B. subtilis* and *E. coli*.

S. no.	Name of the organism	BPE-FeNPs	BPE	Zone of inhibition (mm in diameter)			
				SLE-FeNPs	SLE	PC-1	PC-2
1	<i>B. subtilis</i>	22.70 ± 0.40	—	23.56 ± 1.00	8.25 ± 0.75	17.45 ± 1.67	18.45 ± 1.67
2	<i>E. coli</i>	20.45 ± 1.66	—	20.33 ± 0.58	06.10 ± 1.56	19.09 ± 0.50	20.60 ± 0.50

BPE-FeNPs: banana peel extract-derived iron nanoparticles; BPE: banana peel extract; SLE-FeNPs: spinach leaf extract-derived iron nanoparticles; SLE: spinach leaf extract; PC-1: positive control (tetracycline); PC-2: positive control (gentamicin); —: no antibacterial activity.

of the most intense peak, and θ is the most intense peak's Bragg angle. The crystallite size was calculated using this equation to be 2.44 nm. The unassigned peaks on the XRD pattern could indicate the crystallization of the extract's bio-natural phase. This is due to some banana peel extracts being adsorbed onto the formed iron NPs, which act as capping and stabilizing agents, preventing Fe from oxidation. The XRD results for *Tridax procumbens* leaf extract, used to make pure Fe_3O_4 with a spinal structure, are quite similar [56]. FeNPs produced by reduction with green tea [57] and sorghum bran [29] extracts were also found to be amorphous, according to recent reports.

3.6. Antibacterial Potential. The antibacterial potential of biogenic iron NPs synthesized from BPE and SLE extracts against *B. subtilis* and *E. coli* was investigated in this study. Table 2 shows the inhibition zone (mm in diameter). BPE-FeNPs have antibacterial properties against *B. subtilis* (22.70 ± 0.40) and *E. coli* (20.45 ± 1.66), whereas SLE-FeNPs have antibacterial properties against *B. subtilis* (23.56 ± 1.00) and *E. coli* (20.33 ± 0.58). Between BPE-FeNPs and SLE-FeNPs, there were no significant differences in antibacterial activities. Tetracycline and gentamicin, both standard antibiotics, were used as positive controls at $5 \mu\text{g}/\text{disk}$ and found the inhibitory activity against *B. subtilis* with a zone of inhibition (mm) 17.45 ± 1.67 and 19.09 ± 0.50 and 18.45 ± 1.67 and 20.60 ± 0.50 against *E. coli* pathogens.

FeNPs are an excellent material for use as antibacterial agents against pathogenic bacterial species, according to the findings. Similar results were also reported for photosynthesis silver and gold NPs [53, 58–62], zinc NPs [63, 64], iron NPs [65, 66], and selenium NPs [67]. Even though NPs are widely used as antimicrobials, little is known about their mechanism. Antimicrobial mechanisms include interfering with cell wall synthesis, inhibiting protein synthesis, interfering with nucleic acid synthesis, and inhibiting a metabolic pathway [35, 68, 69]. It is also reported that these NPs penetrate the microbial membrane and create leakage of electrolytes, ultimately causing cell death. Nanomaterials can increase cell membrane permeability within the bacterial cell, interfere with DNA replication, denature bacterial proteins, and release silver ions [70].

3.7. In Vivo Toxicity Evaluation of SLE- and BPE-Derived FeNPs on *Drosophila melanogaster*. The purpose of this study was to investigate the impact of SLE- and BPE-derived FeNPs on *Drosophila melanogaster* life history characteristics as *in vivo*. For contrast, FeNPs derived from SLE and BPE were mixed in food medium of *Drosophila melanogaster* and some flies were bred on without nanoparticle-mixed food media as a regular diet (control sample). FeNPs were fed to flies at $10 \text{ mg}/\text{L}$ concentrations up to the 1st generation, and 7-day-old flies from the 2nd generation were chosen for this investigation. Fecundity was measured by

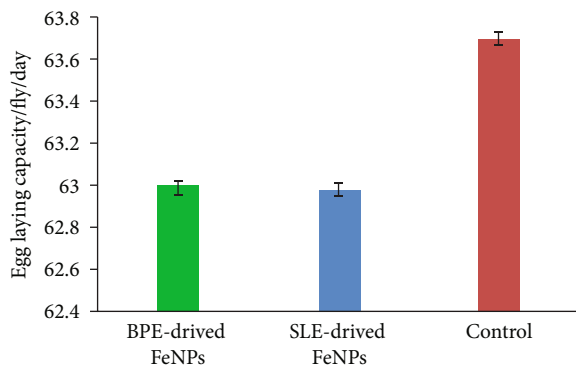


FIGURE 5: Pattern of egg laying capability/fly/day in *D. melanogaster* fed with SLE- and PBE-derived FeNPs and normal diet food (control sample).

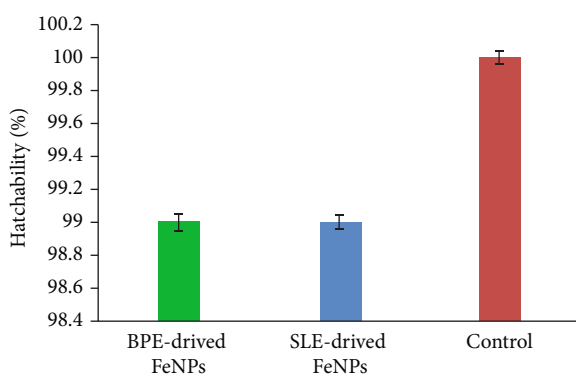


FIGURE 6: Pattern of hatchability (%) in *D. melanogaster* fed with SLE- and PBE-derived FeNPs and normal diet food (control sample).

counting the eggs laid by 7-day-old flies within the 24th hour. The fecundity/fly data clearly demonstrates that the SLE- and BPE-derived FeNPs and control sample had no significant variation in fecundity. The control flies lay 63.70 ± 0.67 eggs/fly/day on average, whereas SLE- and BPE-derived FeNP-fed flies laid 62.98 ± 2.78 and 62.99 ± 2.41 eggs/fly/day, respectively (Figure 5). The obtained results are suggesting that there is no significant difference between normal food and SLE- and BPE-derived FeNP food fed by flies. For hatchability testing, we placed 100 eggs of normal food and FeNP-fed flies in a line pattern on an ethanol-soaked black paper strip (contamination free) on the slant surface of food medium (10×10 eggs/vial). Furthermore, the eggs of normal food-fed flies hatched 100% of the time, but those of the SLE- and BPE-derived FeNPs hatched 99% of the time (Figure 6). These findings again confirm the nontoxic nature of SLE- and BPE-derived FeNPs. Furthermore, the viability (larvae developed into adult fly) of both types of food medium-fed flies was tested. The viability results showed that 100% of adult's emergence in both normal- and FeNP-fed flies (Figure 7). These findings again confirm the nontoxicity of nanoparticles. In continuation, we further investigate any effect of nanoparticles on the duration of development times of *D. melanogaster* fly eggs to adults in hours at 25°C. The time it took for con-

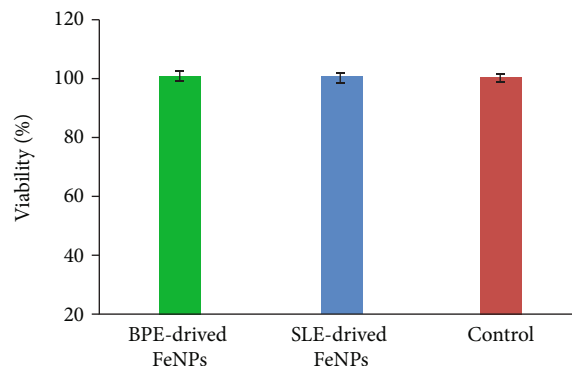


FIGURE 7: Pattern of viability (%) in *D. melanogaster* fed with SLE- and PBE-derived FeNPs and normal diet food (control sample).

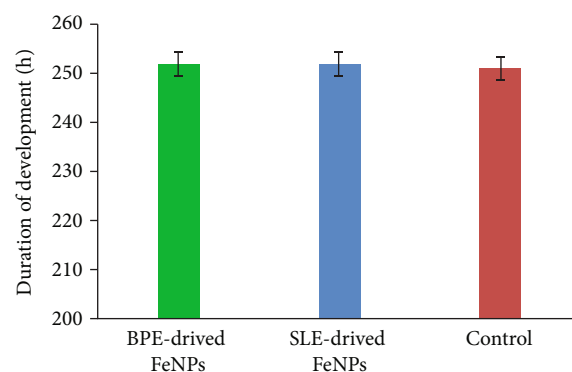


FIGURE 8: Pattern of duration of development (h) in *D. melanogaster* fed with SLE- and PBE-derived FeNPs and normal diet food (control sample).

trol flies to grow eggs to adulthood was 251 hours, whereas SLE- and BPE-derived FeNP-treated flies take one hour extra, i.e., 252 hours (Figure 8). This finding again confirms the nontoxic nature of FeNPs. Similar findings were found by other researchers [71–73].

4. Conclusion

In this research, spinach leaf extract and banana peel are considered for the production of iron NPs. The synthesized NPs were confirmed using visual screening, UV-Vis analysis, FTIR analysis, and XRD analysis. FeNPs were also investigated using size and morphology using TEM. The synthesized green NPs showed antimicrobial activity against the two most common food-borne bacteria, i.e., *B. subtilis* and *E. coli*. Green FeNP impact as *in vivo* toxicity on *D. melanogaster* was evaluated on fecundity, hatchability, viability, and DOD traits after feeding FeNP concentration of 10 mg/L and compared to the normal diet-fed flies (control sample). After evaluating all of the life history traits, we concluded that green-synthesized FeNPs are nontoxic in nature. Overall, FeNPs show a considerable antibacterial potential and might be utilized as antibacterial agents against pathogenic bacteria while maintaining nontoxicity to humans.

Data Availability

The data used to support the findings of this study are available from the corresponding author upon request.

Conflicts of Interest

The authors declare that they have no conflicts of interest.

Acknowledgments

For funds, Author ST is grateful to CST, Uttar Pradesh [Grant no: CST/8276 (Young Scientist Scheme)]. Author SG is also appreciative of the Director, HOD, and project guide of this Institute's unwavering support during her PG dissertation period.

References

- [1] G. A. Silva, "Introduction to nanotechnology and its applications to medicine," *Surgical Neurology*, vol. 61, no. 3, pp. 216–220, 2004.
- [2] T. J. Webster, D. Gorth, and D. Rand, "Silver nanoparticle toxicity in drosophila: size does matter," *International Journal of Nanomedicine*, vol. 6, 2011.
- [3] K. Roy and C. K. Ghosh, "Biological synthesis of metallic nanoparticles: a green alternative," in *Nanotechnology: Synthesis to Applications*, pp. 131–145, CRC Press, 2017.
- [4] M. A. Majeed Khan, S. Kumar, M. Ahamed, S. A. Alrokayan, and M. S. AlSalhi, "Structural and thermal studies of silver nanoparticles and electrical transport study of their thin films," *Nanoscale Research Letters*, vol. 6, no. 1, pp. 1–8, 2011.
- [5] S. Panigrahi, S. Kundu, S. K. Ghosh, S. Nath, and T. Pal, "General method of synthesis for metal nanoparticles," *Journal of Nanoparticle Research*, vol. 6, no. 4, pp. 411–414, 2004.
- [6] L. Castillo-Henríquez, K. Alfaro-Aguilar, J. Ugalde-Álvarez, L. Vega-Fernández, G. Montes de Oca-Vásquez, and J. R. Vega-Baudrit, "Green synthesis of gold and silver nanoparticles from plant extracts and their possible applications as antimicrobial agents in the agricultural area," *Nanomaterials*, vol. 10, no. 9, 2020.
- [7] K. Thiyagarajan, V. K. Bharti, S. Tyagi et al., "Synthesis of non-toxic, biocompatible, and colloidal stable silver nanoparticle using egg-white protein as capping and reducing agents for sustainable antibacterial application," *RSC Advances*, vol. 8, no. 41, pp. 23213–23229, 2018.
- [8] S. Tyagi, "Role of phytochemicals on biosynthesis of silver nanoparticles from plant extracts and their concentration dependent toxicity impacts on drosophila melanogaster," *Biological Insights*, vol. 1, pp. 21–28, 2016.
- [9] C. A. Charitidis, P. Georgiou, M. A. Koklioti, A. F. Trompeta, and V. Markakis, "Manufacturing nanomaterials: from research to industry," *Manufacturing Review*, vol. 1, p. 11, 2014.
- [10] H. Şengül, T. L. Theis, and S. Ghosh, "Toward sustainable Nanoproducts," *Journal of Industrial Ecology*, vol. 12, no. 3, pp. 329–359, 2008.
- [11] P. K. Tyagi, M. Mishra, N. Khan, S. Tyagi, and S. Sirohi, "Toxicological study of silver nanoparticles on gut microbial community probiotic," *Environmental Nanotechnology, Monitoring & Management*, vol. 5, pp. 36–43, 2016.
- [12] B. Uzair, A. Liaqat, H. Iqbal et al., "Green and cost-effective synthesis of metallic nanoparticles by algae: safe methods for translational medicine," *Bioengineering*, vol. 7, no. 4, 2020.
- [13] A. I. Usman, A. A. Aziz, and O. A. Noqta, "Application of green synthesis of gold nanoparticles: a review," *Jurnal Teknologi*, vol. 81, no. 1, pp. 171–182, 2018.
- [14] P. K. Tyagi, S. Tyagi, V. Sarsar, and A. Ahuja, "Synthesis of metal nanoparticles: a biological prospective for analysis," *International Journal of Pharmaceutical Innovations*, vol. 2, no. 4, pp. 48–60, 2012.
- [15] S. Senapati, A. Ahmad, M. I. Khan, M. Sastry, and R. Kumar, "Extracellular biosynthesis of bimetallic Au-Ag alloy nanoparticles," *Small*, vol. 1, no. 5, pp. 517–520, 2005.
- [16] T. Klaus, R. Joerger, E. Olsson, and C. G. Granqvist, "Silver-based crystalline nanoparticles, microbially fabricated," *Proceedings of the National Academy of Sciences*, vol. 96, no. 24, pp. 13611–13614, 1999.
- [17] V. Bansal, D. Rautaray, A. Ahmad, and M. Sastry, "Biosynthesis of zirconia nanoparticles using the fungus fusarium oxysporum," *Journal of Materials Chemistry*, vol. 14, no. 22, pp. 3303–3305, 2004.
- [18] P. Mohanpuria, N. K. Rana, and S. K. Yadav, "Biosynthesis of nanoparticles: technological concepts and future applications," *Journal of Nanoparticle Research*, vol. 10, no. 3, pp. 507–517, 2008.
- [19] J. L. Gardea-Torresdey, J. G. Parsons, E. Gomez et al., "Formation and growth of au nanoparticles inside live alfalfa plants," *Nano Letters*, vol. 2, no. 4, pp. 397–401, 2002.
- [20] M. Rai, A. Yadav, and A. Gade, "CRC 675—current trends in phytosynthesis of metal nanoparticles," *Critical Reviews in Biotechnology*, vol. 28, no. 4, pp. 277–284, 2008.
- [21] M. Sathishkumar, K. Sneha, and Y. S. Yun, "Immobilization of silver nanoparticles synthesized using *Curcuma longa* tuber powder and extract on cotton cloth for bactericidal activity," *Bioresource Technology*, vol. 101, no. 20, pp. 7958–7965, 2010.
- [22] H. B. Na, I. C. Song, and T. Hyeon, "Inorganic nanoparticles for MRI contrast agents," *Advanced Materials*, vol. 21, no. 21, pp. 2133–2148, 2009.
- [23] R. Singh and J. W. Lillard, "Nanoparticle-based targeted drug delivery," *Experimental and Molecular Pathology*, vol. 86, no. 3, pp. 215–223, 2009.
- [24] L. Yang, P. W. May, L. Yin, R. Brown, and T. B. Scott, "Direct growth of highly organized crystalline carbon nitride from liquid-phase pulsed laser ablation," *Chemistry of Materials*, vol. 18, no. 21, pp. 5058–5064, 2006.
- [25] K. S. Chou, K. C. Huang, and H. H. Lee, "Fabrication and sintering effect on the morphologies and conductivity of nano-Ag particle films by the spin coating method," *Nanotechnology*, vol. 16, no. 6, pp. 779–784, 2005.
- [26] S. Saif, A. Tahir, and Y. Chen, "Green synthesis of iron nanoparticles and their environmental applications and implications," *Nanomaterials*, vol. 6, no. 11, p. 209, 2016.
- [27] H. B. Rashmi and P. S. Negi, "Health benefits of bioactive compounds from vegetables," in *Plant-Derived Bioactives: Production, Properties and Therapeutic Applications*, pp. 115–166, Springer, Singapore, 2020.
- [28] R. Best, D. A. Lewis, and N. Nasser, "The anti-ulcerogenic activity of the unripe plantain banana (*Musa species*)," *British Journal of Pharmacology*, vol. 82, no. 1, pp. 107–116, 1984.
- [29] E. C. Njagi, H. Huang, L. Stafford et al., "Biosynthesis of iron and silver nanoparticles at room temperature using aqueous

- sorghum bran extracts," *Langmuir*, vol. 27, no. 1, pp. 264–271, 2011.
- [30] A. Jain, F. Ahmad, D. Gola et al., "Multi dye degradation and antibacterial potential of papaya leaf derived silver nanoparticles," *Environmental Nanotechnology, Monitoring & Management*, vol. 14, article 100337, 2020.
- [31] P. K. Tyagi, D. Gola, S. Tyagi et al., "Synthesis of zinc oxide nanoparticles and its conjugation with antibiotic: antibacterial and morphological characterization," *Environmental Nanotechnology, Monitoring & Management*, vol. 14, article 100391, 2020.
- [32] P. K. Tyagi, "Use of biofabricated silver nanoparticles-conjugated with antibiotic against multidrug resistant pathogenic bacteria," *Biological Insights*, vol. 1, no. 1, pp. 1-2, 2016.
- [33] A. Ahuja, R. S. Tanwar, P. K. Tyagi, V. Sarsar, M. Paudwal, and P. Kumar, "Local adaption in life history traits of *Drosophila melanogaster* in extreme conditions of humidity," *International Journal of Animal Biotechnology*, vol. 2, no. 1, pp. 1–5, 2012.
- [34] A. S. Y. Ting and J. E. Chin, "Biogenic synthesis of iron nanoparticles from apple peel extracts for decolorization of malachite green dye," *Water, Air, and Soil Pollution*, vol. 231, no. 6, 2020.
- [35] Y. Zhang, X. Pan, S. Liao et al., "Quantitative proteomics reveals the mechanism of silver nanoparticles against Multidrug-Resistant *Pseudomonas aeruginosa* Biofilms," *Journal of Proteome Research*, vol. 19, no. 8, pp. 3109–3122, 2020.
- [36] O. J. K. Okoth, *Synthesis and characterization of iron nanoparticles using banana peels extracts and their application in apta-sensor*, [Ph.D. thesis], University of Nairobi, 2016.
- [37] C. P. Devatha, A. K. Thalla, and S. Y. Katte, "Green synthesis of iron nanoparticles using different leaf extracts for treatment of domestic waste water," *Journal of Cleaner Production*, vol. 139, pp. 1425–1435, 2016.
- [38] M. I. Din, A. Zahoor, Z. Hussain, and R. Khalid, "A review on green synthesis of iron (Fe) nanomaterials, its alloys and oxides," *Inorganic and Nano-Metal Chemistry*, vol. 53, pp. 1–17, 2020.
- [39] D. S. Amrutha, J. Joseph, C. A. Vineeth, A. John, and A. Abraham, "Green synthesis of *Cuminum cyminum* silver nanoparticles: characterizations and cytocompatibility with lapine primary tenocytes," *Journal of Biosciences*, vol. 46, no. 1, pp. 1–14, 2021.
- [40] A. Bankar, B. Joshi, A. R. Kumar, and S. Zinjarde, "Banana peel extract mediated novel route for the synthesis of silver nanoparticles," *Colloids and Surfaces A: Physicochemical and Engineering Aspects*, vol. 368, no. 1–3, pp. 58–63, 2010.
- [41] A. Bankar, B. Joshi, A. Ravi Kumar, and S. Zinjarde, "Banana peel extract mediated synthesis of gold nanoparticles," *Colloids and Surfaces B: Biointerfaces*, vol. 80, no. 1, pp. 45–50, 2010.
- [42] A. Bankar, B. Joshi, A. R. Kumar, and S. Zinjarde, "Banana peel extract mediated novel route for the synthesis of palladium nanoparticles," *Materials Letters*, vol. 64, no. 18, pp. 1951–1953, 2010.
- [43] B. A. Korgel, S. Fullam, S. Connolly, and D. Fitzmaurice, "Assembly and self-organization of silver nanocrystal superlattices: ordered "soft spheres"," *Journal of Physical Chemistry B*, vol. 102, no. 43, pp. 8379–8388, 1998.
- [44] C. Vidya, S. Hiremath, M. N. Chandraprabha et al., "Green synthesis of ZnO nanoparticles by *Calotropis gigantea*," *International Journal of Current Engineering and Technology*, vol. 1, 2013.
- [45] V. T. Nguyen, "Sunlight-driven synthesis of silver nanoparticles using pomelo peel extract and antibacterial testing," *Journal of Chemistry*, vol. 2020, Article ID 6407081, 9 pages, 2020.
- [46] D. S. Sheny, J. Mathew, and D. Philip, "Phytosynthesis of Au, Ag and Au-Ag bimetallic nanoparticles using aqueous extract and dried leaf of *Anacardium occidentale*," *Spectrochimica Acta-Part A: Molecular and Biomolecular Spectroscopy*, vol. 79, no. 1, pp. 254–262, 2011.
- [47] T. Shahwan, S. Abu Sirriah, M. Nairat et al., "Green synthesis of iron nanoparticles and their application as a Fenton-like catalyst for the degradation of aqueous cationic and anionic dyes," *Chemical Engineering Journal*, vol. 172, no. 1, pp. 258–266, 2011.
- [48] R. P. Singh, V. K. Shukla, R. S. Yadav, P. K. Sharma, P. K. Singh, and A. C. Pandey, "Biological approach of zinc oxide nanoparticles formation and its characterization," *Advanced Materials Letters*, vol. 2, no. 4, pp. 313–317, 2011.
- [49] M. Hazaa, M. Alm-Eldin, A. E. Ibrahim et al., "Biosynthesis of silver nanoparticles using *Borago officinalis* leaf extract, characterization and larvicidal activity against cotton leaf worm, *Spodoptera littoralis* (Bosid)," *International Journal of Tropical Insect Science*, vol. 41, no. 1, pp. 145–156, 2021.
- [50] R. Jain, S. Mendiratta, L. Kumar, and A. Srivastava, "Green synthesis of iron nanoparticles using *Artocarpus heterophyllus* peel extract and their application as a heterogeneous Fenton-like catalyst for the degradation of Fuchsin basic dye," *Current Research in Green and Sustainable Chemistry*, vol. 4, article 100086, 2021.
- [51] O. P. Bolade, A. B. Williams, and N. U. Benson, "Green synthesis of iron-based nanomaterials for environmental remediation: a review," *Environmental Nanotechnology, Monitoring & Management*, vol. 13, article 100279, 2020.
- [52] S. Tyagi, A. Kumar, and P. K. Tyagi, "Comparative analysis of metal nanoparticles synthesized from *Hibiscus ROSA SINESIS* and their antibacterial activity estimation against nine pathogenic bacteria," *Asian Journal of Pharmaceutical and Clinical Research*, vol. 10, no. 5, pp. 323–329, 2017.
- [53] S. Tyagi, P. K. Tyagi, D. Gola, N. Chauhan, and R. K. Bharti, "Extracellular synthesis of silver nanoparticles using entomopathogenic fungus: characterization and antibacterial potential," *SN Applied Sciences*, vol. 1, no. 12, p. 1545, 2019.
- [54] G. Sathishkumar, V. Logeshwaran, S. Sarathbabu et al., "Green synthesis of magnetic Fe_3O_4 nanoparticles using *Couroupita guianensis* Aubl. fruit extract for their antibacterial and cytotoxicity activities," *Artificial Cells, Nanomedicine and Biotechnology*, vol. 46, no. 3, pp. 589–598, 2018.
- [55] M. Fazlzadeh, R. Khosravi, and A. Zarei, "Green synthesis of zinc oxide nanoparticles using *Peganum harmala* seed extract, and loaded on *Peganum harmala* seed powdered activated carbon as new adsorbent for removal of Cr(VI) from aqueous solution," *Ecological Engineering*, vol. 103, pp. 180–190, 2017.
- [56] C. Ramesh, K. T. Mohan Kumar, N. Latha, and V. Ragunathan, "Green synthesis of Cr_2O_3 nanoparticles using *Tridax procumbens* leaf extract and its antibacterial activity on *Escherichia coli*," *Digest Journal of Nanomaterials and Biostructures*, vol. 8, no. 4, pp. 603–607, 2012.
- [57] M. N. Nadagouda, A. B. Castle, R. C. Murdock, S. M. Hussain, and R. S. Varma, "In vitro biocompatibility of nanoscale zero-valent iron particles (NZVI) synthesized using tea polyphenols," *Green Chemistry*, vol. 12, no. 1, pp. 114–122, 2010.

- [58] M. C. D. Niluxsshun, K. Masilamani, and U. Mathiventhan, "Green Synthesis of Silver Nanoparticles from the Extracts of Fruit Peel of Citrus tangerina, Citrus sinensis, and Citrus limon for Antibacterial Activities," *Bioinorganic Chemistry and Applications*, vol. 2021, no. 1, 8 pages, 2021.
- [59] S. A. Akintelu, B. Yao, and A. S. Folorunso, "Green synthesis, characterization, and antibacterial investigation of synthesized gold nanoparticles (AuNPs) from Garcinia kola pulp extract," *Plasmonics*, vol. 16, no. 1, pp. 157–165, 2021.
- [60] Z. Qiusheng and M. Jun, "Reactive oxygen species and morphine addiction," in *Reactive Oxygen Species in Biology and Human Health*, pp. 501–512, CRC Press., 2017.
- [61] P. K. Tyagi, R. Mishra, F. Khan, D. Gupta, and D. Gola, "Antifungal effects of silver nanoparticles against various plant pathogenic fungi and its safety evaluation on *Drosophila melanogaster*," *Biointerface Research in Applied Chemistry*, vol. 10, no. 6, pp. 6587–6596, 2020.
- [62] P. K. Tyagi, M. Mishra, N. Khan, and S. Tyagi, "Antibacterial activity and toxicological evaluation of silver nanoparticles through ToxTrak toxicity test," *International Journal of Current Microbiology and Applied Sciences*, vol. 4, no. 3, pp. 1043–1055, 2015.
- [63] S. Sirohi and P. K. Tyagi, "Synthesis and synergistic effects of ciprofloxacin conjugated zinc oxide nanoparticles," *Online*, vol. 9, 2019.
- [64] J. P. Shabaaz Begum, K. Manjunath, S. Pratibha, N. Dhananjaya, P. Sahu, and S. Kashaw, "Bioreduction synthesis of zinc oxide nanoparticles using *Delonix regia* leaf extract (Gul Mohar) and its agromedicinal applications," *Journal of Science: Advanced Materials and Devices*, vol. 5, no. 4, pp. 468–475, 2020.
- [65] S. Saranya, K. Vijayarani, and S. Pavithra, "Green synthesis of iron nanoparticles using aqueous extract of *Musa ornata* flower sheath against pathogenic bacteria," *Indian Journal of Pharmaceutical Sciences*, vol. 79, no. 5, pp. 688–694, 2017.
- [66] Y. Vitta, M. Figueroa, M. Calderon, and C. Ciangherotti, "Synthesis of iron nanoparticles from aqueous extract of *Eucalyptus robusta* Sm and evaluation of antioxidant and antimicrobial activity," *Materials Science for Energy Technologies*, vol. 3, pp. 97–103, 2020.
- [67] S. Menon, H. Agarwal, S. Rajeshkumar, P. Jacqueline Rosy, and V. K. Shanmugam, "Investigating the antimicrobial activities of the biosynthesized selenium nanoparticles and its statistical analysis," *Bionanoscience*, vol. 10, no. 1, pp. 122–135, 2020.
- [68] F. C. Tenover, "Mechanisms of antimicrobial resistance in bacteria," *American Journal of Medicine*, vol. 119, no. 6, pp. S3–S10, 2006.
- [69] E. Sanders and L. E. Cluff, "Mechanisms of action of antimicrobial agents," vol. 15, 1968.
- [70] P. K. Tyagi, P. Upadhyay, P. Kaul, S. Chaudhary, and E. Mansi Mishra, "Detection of routes of interaction between silver nanoparticles and bacterial cell membrane," *International Journal of Basic and Applied Biology*, vol. 3, no. 2, pp. 111–114, 2016.
- [71] N. Ahamad, P. Bhardwaj, E. Bhatia, and R. Banerjee, "Clinical toxicity of nanomedicines," in *Nano Medicine and Nano Safety*, pp. 533–560, Springer, 2020.
- [72] A. O. Abolaji, K. D. Fasae, C. E. Iwezor, M. Aschner, and E. O. Farombi, "Curcumin attenuates copper-induced oxidative stress and neurotoxicity in *Drosophila melanogaster*," *Toxicology Reports*, vol. 7, pp. 261–268, 2020.
- [73] B. O. Oyetayo, A. O. Abolaji, K. D. Fasae, and A. Aderibigbe, "Ameliorative role of diets fortified with curcumin in a *Drosophila melanogaster* model of aluminum chloride-induced neurotoxicity," *Journal of Functional Foods*, vol. 71, article 104035, 2020.